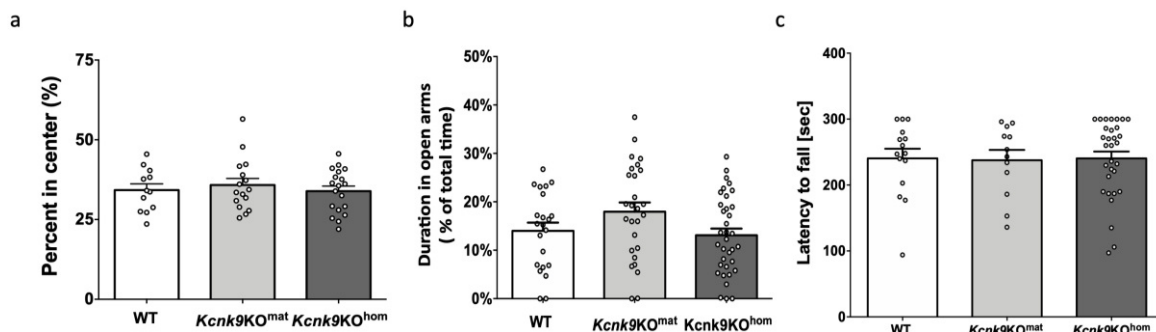


Supplementary Information

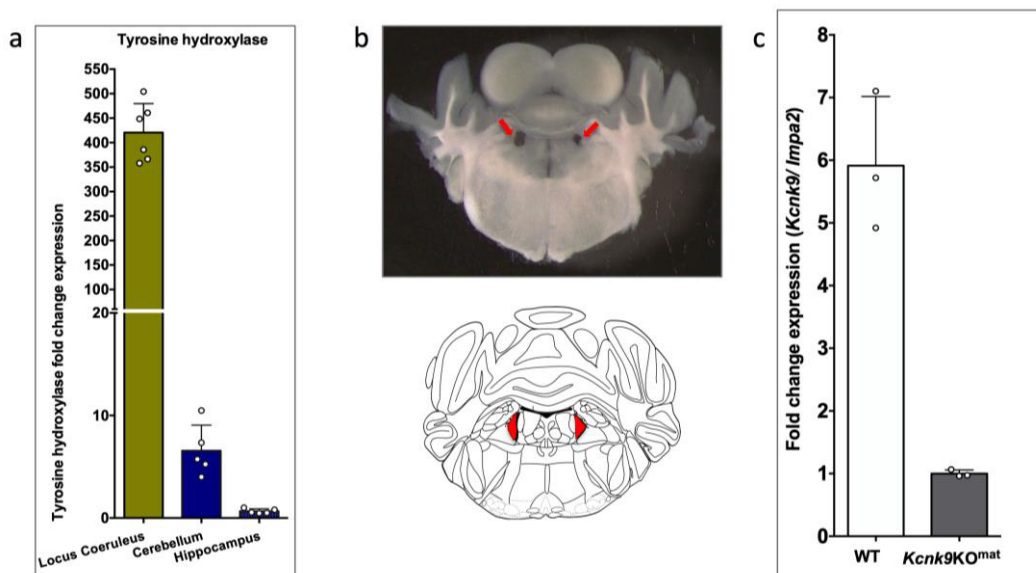
**Inhibition of histone deacetylation rescues phenotype in a mouse model of Birk-Barel
Intellectual Disability syndrome**

Cooper et al.

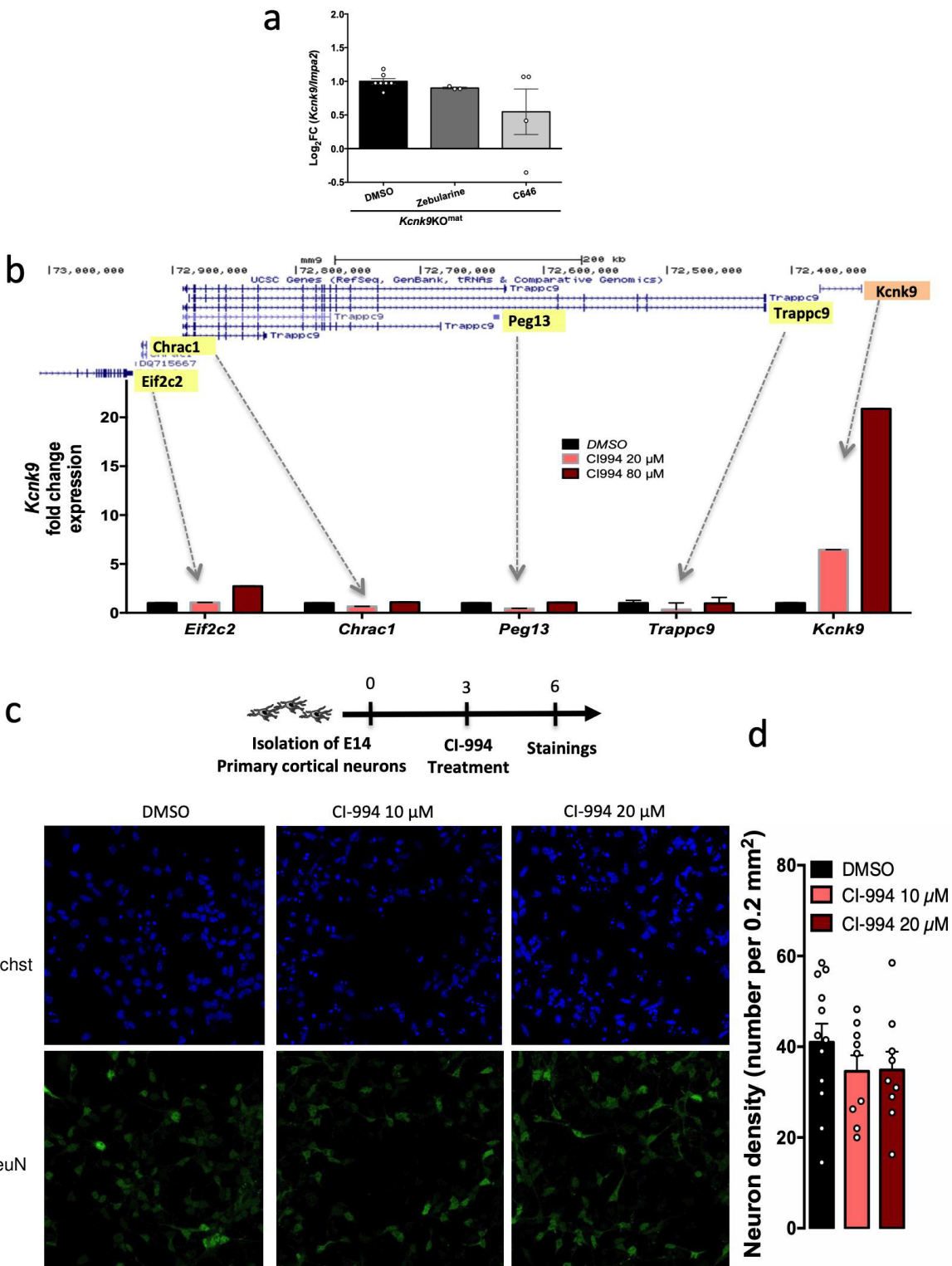
Supplementary Figures



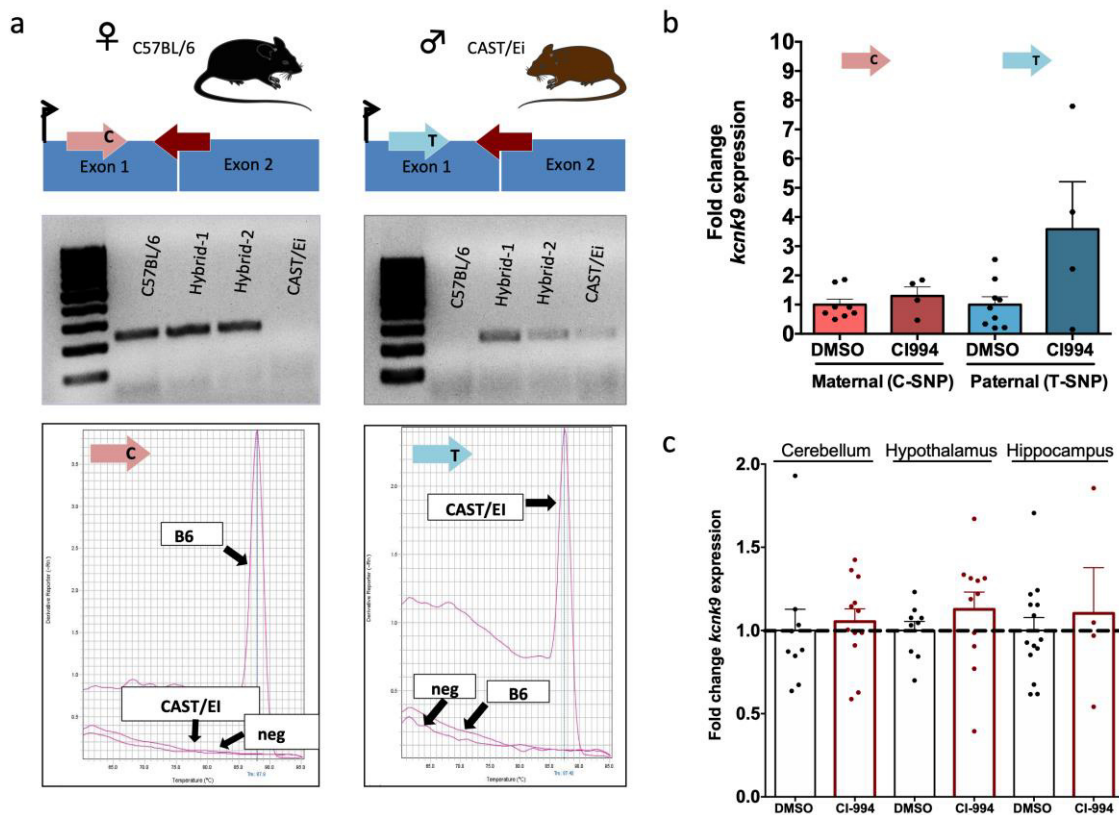
Supplementary Figure 1: Deletion of *Kcnk9* does not affect anxiety and motor coordination of *Kcnk9KO* mice. No significant differences were observed in (a) the open-field-test between WT (n=12), *Kcnk9KO^{mat}* (n=16) and *Kcnk9KO^{hom}* (n=19) mice, (b) the elevated-plus-maze between WT (n=22), *Kcnk9KO^{mat}* (n=27) and *Kcnk9KO^{hom}* (n=35) mice, and (c) the rotarod-test between WT (n=15), *Kcnk9KO^{mat}* (n=12) and *Kcnk9KO^{hom}* (n=31) mice using One-way ANOVA and followed Bonferroni's multiple comparison post hoc test. Values are means \pm SEM. (a-c) Behavioral data are from biologically independent animals (n= number of mice). Statistical analyses and approaches are provided in Supplementary Table 1. Source data are provided as a Source Data file.



Supplementary Figure 2: Locus coeruleus expression analysis (a) Tyrosine hydroxylase (TH) RT-qPCR expression analysis. The TH expression was highly increased in locus coeruleus (LC, n=6) compared to cerebellum (n=5) and hippocampus (n=5) samples of WT mice. TH serves as a norepinephrine marker. (b) Coronal brain slice of an adult mouse; red arrows indicate tissue excision position of LC (top) schematic coronal section of the mouse brain at the position -5.4 relative to bregma¹; LC is depicted as a red triangle (bottom) (c) *Kcnk9* RT-qPCR expression analysis in LC samples of WT (n=3) compared to those of *Kcnk9KO^{mat}* (n=3) mice. (a,c) n= biologically independent samples from individual mice. Values are means \pm SEM. Source data are provided as a Source Data file.

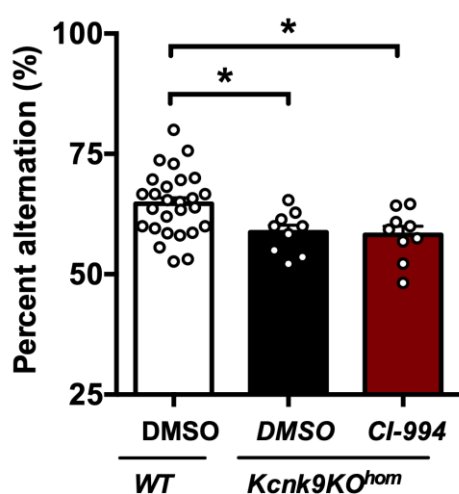


Supplementary Figure 3: Epigenetic drug treatments in murine primary cortical neurons (mPCNs). (a) The compounds Zebularine and C646 show no effect on the *Kcnk9* expression in *Kcnk9KO^{mat}* mPCNs (Zebularine P=0.0667, C646 P=0.4727, Mann-Whitney-U test). (b) RT-qPCR expression analysis of known genes in the imprinting cluster on mouse chromosome 15. CI-994 treatment (20 μ M and 80 μ M CI-994) did not affect expression of *Trappc9*, *Peg13*, *Chrac1* and *Eif2c2* in mPCNs (n=2-3 cultures/group). (c) Evaluation of toxicity/viability in CI-994 treated mPCN compared to DMSO-treated controls. Cells were stained with Hoechst 33258 (nucleus) and NeuN (mature neurons) 3 days after treatment with either DMSO or CI-994. (d) Neuron density after CI-994 treatment. No significant difference in neuronal density was observed between DMSO (n=12), 10 μ M CI-994 (n=9) and 20 μ M CI-994 (n=9) treated mPCNs. Values are means \pm SEM. Statistical analyses and approaches are provided in Supplementary Table 1. Source data are provided as a Source Data file.

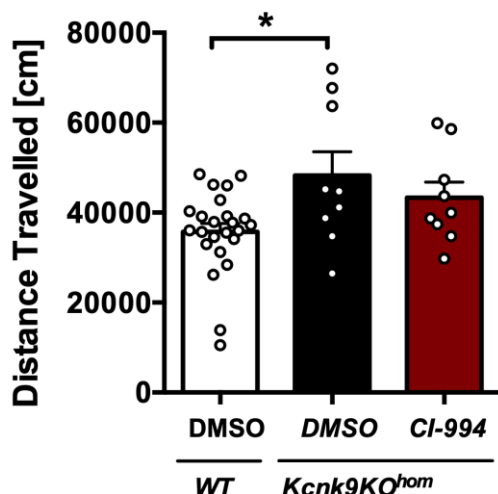


Supplementary Figure 4: Allele-specific de-repression of *Kcnk9* in the mouse brain **(a)** Assay design and melt curve analysis for the allele-specific RT-qPCR (AS-RT-qPCR) of *Kcnk9*. Allele-specific primers bind to the strain-specific SNP at the 3'-end, allowing only the complementary primer to elongate (top). Agarose gel electrophoresis of PCR product (231 bp) loaded on 2% agarose gel using a 100 bp DNA ladder (middle). Melt curve analysis shows a primer-specific binding (bottom). **(b)** Analysis of expression levels using the C57BL/6 C and Cast/Ei T allele-specific primer and normalization with a reference gene revealed an increased expression of the paternal *Kcnk9* allele in the hippocampus in *Kcnk9KO^{mat}* hybrid mice treated with CI-994 (n= 4) compared to *Kcnk9KO^{mat}* DMSO controls (n= 8). No difference between the maternal *Kcnk9* allele expression comparing DMSO (n= 9) and CI-994 (n=4) treated mice **(c)** Gene expression of *Kcnk9* in WT mice treated with DMSO compared to CI-994 treated mice shows no significant differences in several analysed brain regions. WT cerebellum (DMSO n= 9, CI-994 n=12), hypothalamus (DMSO n= 9, CI-994 n= 11) and hippocampus (DMSO n=14, CI-994 n=4). Mann-Whitney U. Values are means \pm SEM. Statistical analyses and approaches are provided in Supplementary Table 1. Source data are provided as a Source Data file. Components of this figure were created using Servier Medical Art templates, which are licensed under a Creative Commons Attribution 3.0 Unported License; <https://smart.servier.com>.

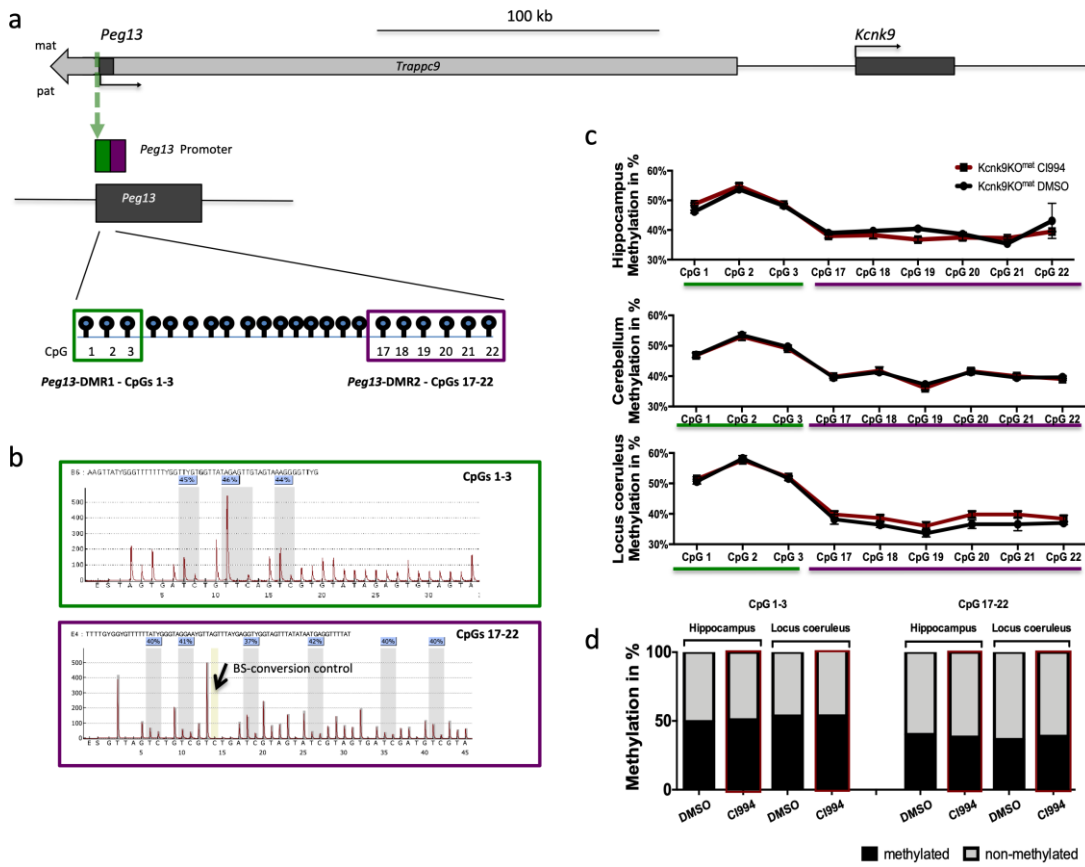
a



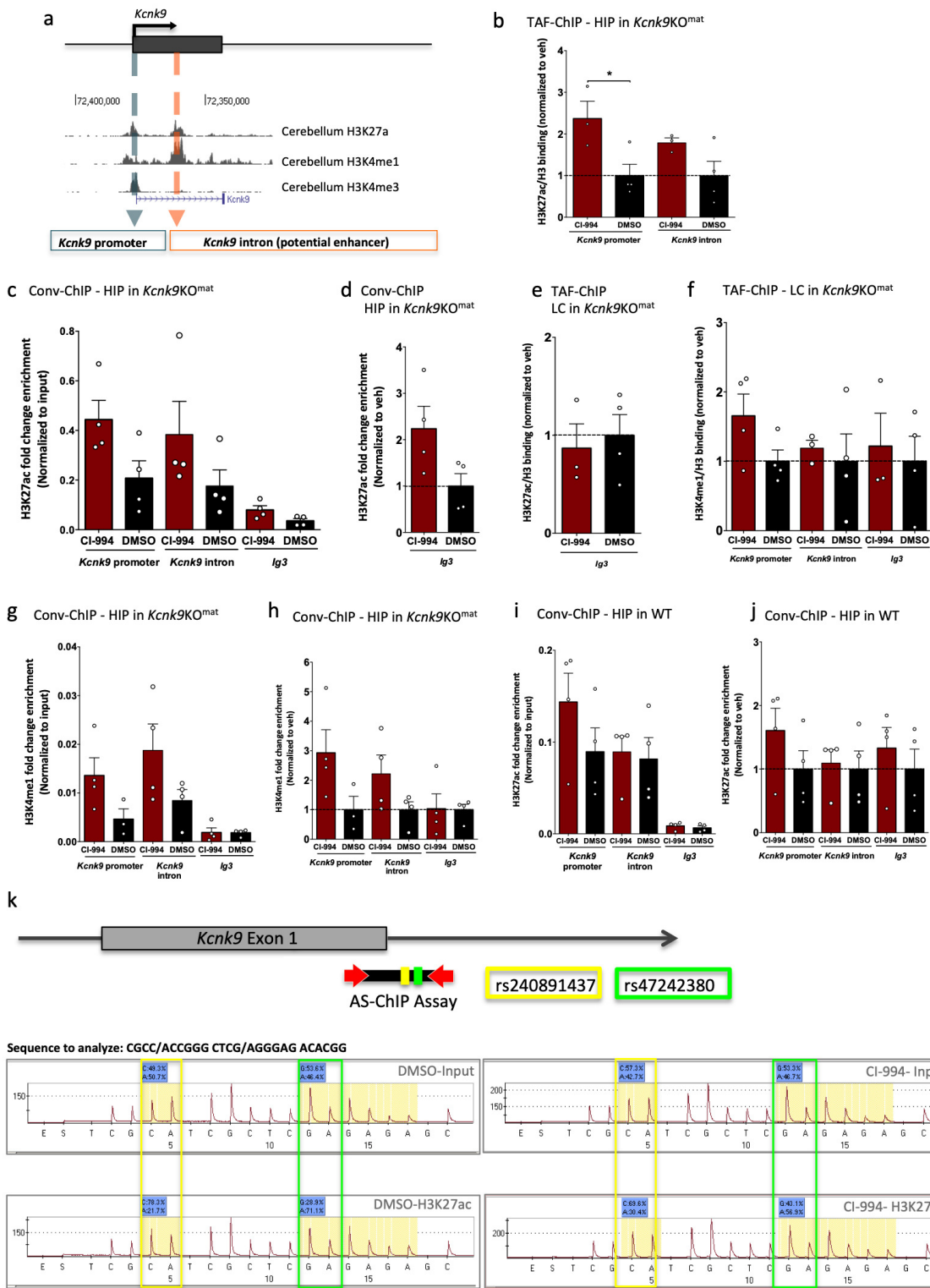
b



Supplementary Figure 5: No behavioural rescue of *Kcnk9KO^{hom}* mice after CI-994 treatment. (a) Y-maze percentage alternation analysis of DMSO-treated WT (n=27), DMSO-treated *Kcnk9KO^{hom}* (n=9) and CI994-treated *Kcnk9KO^{hom}* (n=9) treated mice. DMSO- and CI-994-treated *Kcnk9KO^{hom}* mice display a significant decrease in percentage alteration compared to WT mice. One-way ANOVA: $F(2, 39) = 4.710, P = 0.0147$; followed by Bonferroni's multiple comparison post hoc test, * $P < 0.05$. (b) Total locomotor activity in dark (12h) phase reveals no significant difference between DMSO-treated *Kcnk9KO^{hom}* (n=9) and CI-994-treated *Kcnk9KO^{hom}* (n=9) treated mice. A significant difference was observed by comparing DMSO-treated WT (n=24) and *Kcnk9KO^{hom}* mice. One-way ANOVA: $F(2, 42) = 5.569, P = 0.0072$; followed by Bonferroni's multiple comparison post hoc test, * $P < 0.05$. (a-b) Behavioral data are from biologically independent animals (n= number of mice). Values are means \pm SEM Statistical analyses and approaches are provided in Supplementary Table 1. Source data are provided as a Source Data file.



Supplementary Figure 6: CI-994 treatment of *Kcnk9KO^{mat}* mice does not interfere with DNA methylation at the *Peg13*-DMR. (a) Schematic presentation of the *Kcnk9* and *Peg13* loci on distal mouse chromosome 15. The *Peg13* differentially methylated region (*Peg13*-DMR) is analyzed in two separate assays. *Peg13*-DMR1 (green) and *Peg13*-DMR2 (violet). Individual CpGs analysed are depicted as lollipops. (b) The pyrogram shows the methylation status of the *Peg13*-DMRs in the hippocampus. The Y-axis shows the intensity of the light emission. The X-axis shows the dispensing order of the added nucleotides. The CpGs are highlighted in gray. In the blue box, the percentage of methylation is given. The bisulfite conversion control is highlighted in yellow. (c,d) CI-994 did not significantly alter the DNA methylation status of *Peg13*-DMR1 (CpGs 1-3) and *Peg13*-DMR2 (CpGs 17-22) in hippocampus, cerebellum or locus coeruleus measured using the bisulfite pyrosequencing method, n=3-5 DNA samples/ group, biologically independent animals. Values are means \pm SEM. Statistical analyses and approaches are provided in Supplementary Table 1. Source data are provided as a Source Data file.



Supplementary Figure 7: CI-994 treatment of *Kcnk9KO^{mat}* mice affects histone modifications at the *Kcnk9* locus. (a) Schematic presentation of *Kcnk9* on distal mouse chromosome 15. The murine *Kcnk9* gene is shown with the corresponding H3K27ac, H3K4me1 and H3K4me3 peaks (UCSC Genome Browser on Mouse July 2007 (NCBI37/mm9) Assembly). (b) TAF-ChIP-qPCR of H3K27ac marks at the promoter and intronic region of *Kcnk9* in the hippocampus of *Kcnk9KO^{mat}* animals following treatment with CI-994 (normalized to veh), *Kcnk9* promoter: P = 0.0342, and *Kcnk9* intron P = 0.1172, each DMSO vs. CI-994 (c) TAF-ChIP-qPCR of H3K27ac marks at the promoter and intronic region of *Kcnk9* in the hippocampus of *Kcnk9KO^{mat}* animals following treatment with CI-994 (% of input). Related to figure 6b. (d) H3K27ac enrichment at intergenic control region in the hippocampus of *Kcnk9KO^{mat}* animals following treatment with CI-994 (normalized to veh). Related to figure 6b and suppl. figure 8c. (e) H3K27ac enrichment (norm to H3) at intergenic control region in the locus coeruleus of *Kcnk9KO^{mat}* animals following treatment with CI-994 (normalized to veh). Related to figure 6b. (f) TAF-ChIP-qPCR of H3K4me1 marks at the promoter and intronic region of *Kcnk9* in locus coeruleus of *Kcnk9KO^{mat}* animals following treatment with CI-994 (normalized to veh). Related to figure 6b. (g) Conv-ChIP - HIP in *Kcnk9KO^{mat}* animals following treatment with CI-994 (normalized to input). (h) Conv-ChIP - HIP in *Kcnk9KO^{mat}* animals following treatment with CI-994 (normalized to veh). (i) Conv-ChIP - HIP in WT mice following treatment with CI-994 (normalized to input). (j) Conv-ChIP - HIP in WT mice following treatment with CI-994 (normalized to veh). (k) AS-ChIP assay schematic showing sequencing primers rs240891437 and rs47242380 flanking the Kcnk9 exon 1 region."/>

treatment with CI-994 (normalized to veh). **(g-h)** Conventional ChIP-qPCR of H3K4me1 marks at the promoter and intronic region of *Kcnk9* in the hippocampus of *Kcnk9KO^{mat}* animals following treatment with CI-994 presented as (g) % of input and (h) normalized to veh. **(i-j)** Conventional ChIP-qPCR of H3K27ac marks at the promoter and intronic region of *Kcnk9* in the hippocampus of wildtype C57BL/6 animals following treatment with CI-994 presented as (i) % of input and (j) normalized to veh. **(b-j)** Values are means ± SEM, Student's t-test; (n=3-4 animals/group). n= 3-4 samples/group, biologically independent animals. Data per plot was generated in 2 independent experiments. **(k)** Allele-specific ChIP-qPCR. The pyrogram shows the status of SNPs rs240891437 and rs47242380 in the intronic region of *Kcnk9* in the hippocampus. The Y-axis shows the intensity of the light emission. The X-axis shows the dispensing order of the added nucleotides. In the blue box, the percentage of the nucleotide arising from maternal and paternal allele is given. Statistical analyses and approaches are provided in Supplementary Table 1. Source data are provided as a Source Data file.

Supplementary Table 1: Summary of statistical analyses and approaches

Subject	Figure	Genotype	Mean ± SEM	Factor	n	Statistics	Interaction	F value	P value	post hoc	adjusted p-values
Y-maze alteration	1b	WT	64.31 ± 1.619		23	one way ANOVA		F (2, 91) = 7.261	P=0.0012	Bonferroni's multiple comparisons test	**P<0.01 (WT vs. <i>Kcnk 9KO</i> ^{mat})
		<i>Kcnk 9KO</i> ^{mat}	56.62 ± 1.438		27					*P<0.05 (WT vs. <i>Kcnk 9KO</i> ^{hom})	
		<i>Kcnk 9KO</i> ^{hom}	59.02 ± 1.020		44						
Circadian Rhythm	1c	WT	22685 ± 2059		13	one way ANOVA		F (2, 29) = 2.281	P = 0.1203	Bonferroni's multiple comparisons test	n.s.
		<i>Kcnk 9KO</i> ^{mat}	29678 ± 3623	Light phase	10						
		<i>Kcnk 9KO</i> ^{hom}	30978 ± 3817		9						
		WT	38741 ± 2384		18						*P<0.05 (WT vs. <i>Kcnk 9KO</i> ^{mat})
QUASEP	1d	<i>Kcnk 9KO</i> ^{mat}	48170 ± 2457	Dark phase	13	one way ANOVA		F (2, 43) = 22.70	P < 0.0001	Bonferroni's multiple comparisons test	****P<0.0001 (WT vs. <i>Kcnk 9KO</i> ^{hom})
		<i>Kcnk 9KO</i> ^{hom}	61800 ± 2627		15						*P<0.01 (<i>Kcnk 9KO</i> ^{mat} vs. <i>Kcnk 9KO</i> ^{hom})
		96,12142	± 0,171	Cerebellum	14						
		99,15	± 0,298	Pons	10						
		96,225	± 1,541	Olfactory bulb	12						
		93,22143	± 0,334	Cortex	14						
		Maternal expression of (C57BL/6xCast/Ei)F1	99,45715	± 0,204	Hippocampus	14					
		98,43333	± 0,358	Hypothalamus	9						
		95,28	± 0,360	Striatum	5						
		99,06	± 0,434	Midbrain	5						
Open field (percent in center)	Suppl. 1a	98,38	± 0,450	Medulla	5	one way ANOVA		F (2, 44) = 0.3167	P = 0.7302	Bonferroni's multiple comparisons test	n.s.
		86,5	± 1,843	Locus coeruleus	4						
		3,939	± 0,154	Cerebellum	14						
		0,850	± 0,298	Pons	10						
		3,775	± 1,541	Olfactory bulb	12						
		6,750	± 0,314	Cortex	14						
		Paternal expression of (C57BL/6xCast/Ei)F1	0,543	± 0,204	Hippocampus	14					
		1,567	± 0,358	Hypothalamus	9						
		4,720	± 0,360	Striatum	5						
		0,940	± 0,434	Midbrain	5						
Elevated plus maze (duration in open arms)	Suppl. 1b	1,620	± 0,450	Medulla	5	one way ANOVA		F (2, 81) = 2.568	P = 0.0829	Bonferroni's multiple comparisons test	n.s.
		13,500	± 1,843	Locus coeruleus	4						
		WT	14.00 ± 1.704		12						
Rotarod (Latency to fall)	Suppl. 1c	<i>Kcnk 9KO</i> ^{mat}	17.97 ± 1.895		27	one way ANOVA		F (2, 55) = 0.01168	P = 0.9884	Bonferroni's multiple comparisons test	n.s.
		<i>Kcnk 9KO</i> ^{hom}	13.11 ± 1.361		35						
		WT	240.5 ± 14.59		15						
relative <i>Kcnk9</i> expression after knock-down	Fig. 2b	<i>Kcnk 9KO</i> ^{mat}	237.6 ± 15.72		12	one way ANOVA		F (2, 55) = 0.01168	P = 0.9884	Bonferroni's multiple comparisons test	n.s.
		<i>Kcnk 9KO</i> ^{hom}	240.4 ± 10.49		31						
		shRNA 1	0,250		1						
		shRNA 2	0,080		1						
		shRNA 3	0,110		1						
		shRNA 4	0,070		1						
		shRNA 5	0,160		1						
		shRNA 6	0,030		1						
		shRNA 7	0,060		1						
		shRNA 8	0,040		1						
Tyrosine hydroxylase expression	Fig. 2c	shRNA 9	0,050		1			F (2, 55) = 0.01168	P = 0.9884	Arithmetic means of <i>Kcnk9</i> expression of presented IDs were provided by Sirion Biotech	
		shRNA 10	0,060		1						
		negative control	1,000		1						
		WT scrambled control	1.000 ± 0.05220	PFC	8					n.s.	
		WT <i>kcnk9</i> knock-down	1.031 ± 0.04726		4						
		WT scrambled control	1.000 ± 0.08301	Hippocampus	7	Mann-Whitney U (Two-tailed)		F (2, 55) = 0.01168	P = 0.9884		
		WT <i>kcnk9</i> knock-down	0.9579 ± 0.06216		4						
		WT scrambled control	1.000 ± 0.1570	Locus coeruleus	7						
		WT <i>kcnk9</i> knock-down	0.2067 ± 0.08371		4						
		WT scrambled control	1.148 ± 0.1343	Locus coeruleus	7					n.s.	
		WT <i>kcnk9</i> knock-down	1.000 ± 0.1703		4						

Circadian Rhythm	Fig. 2d	WT scrambled control WT <i>kcnk9</i> knock-down	78517 ± 5343 105984 ± 6699	Dark phase	9 10	Mann-Whitney U (Two-tailed)	P=0,0101
Y-maze alteration	Fig. 2e	WT scrambled control WT <i>kcnk9</i> knock-down	60.44 ± 2.352 53.20 ± 4.002		9 10	Mann-Whitney U (Two-tailed)	P=0,0797
Tyrosine hydroxylase expression	Suppl. 2a		420,600 ± 24,150	LC	6		Locus Coeruleus vs. Cerebellum ****P < 0.0001
		<i>Kcnk9KO</i> ^{mat}	6,562 ± 1,117	Cerebellum	5	one way ANOVA	F (2, 13) = 242.0 Locus Coeruleus vs. Hippocampus ****P < 0.0001
			0,664 ± 0,1037	Hippocampus	5		Cerebellum vs. Hippocampus
<i>Kcnk9</i> expression	Suppl. 2c	<i>Kcnk9KO</i> ^{mat} WT	1,000 ± 0,637 5,914 ± 0,033	LC	3 3	Mann-Whitney U (Two-tailed)	P=0,1000
Mean frequency	3d	WT <i>Kcnk9KO</i> ^{mat} <i>Kcnk9KO</i> ^{hom} WT <i>Kcnk9KO</i> ^{mat} <i>Kcnk9KO</i> ^{hom}	2,383 ± 0,153 2,593 ± 0,181 2,350 ± 0,258 3,265 ± 0,256 2,640 ± 0,284 3,799 ± 0,295	day day day night night night	46 41 22 23 26 30	Z-way-ANOVA	Interaction F (2, 182) = 4.435 P = 0.0132 Light Phase: <i>Kcnk9KO</i> ^{mat} vs. Dark phase: <i>Kcnk9KO</i> ^{hom} **P<0.01 Phase F (1, 182) = 16.93 P < 0.0001 Bonferroni's multiple comparisons test Dark phase: <i>Kcnk9KO</i> ^{mat} vs. Dark phase: <i>Kcnk9KO</i> ^{hom} *P<0.05 Genotype F (2, 182) = 1.836 P = 0.1624
Cortical neurons all drugs	4c		1.000 ± 0.0417 3.853 ± 0.3724 <i>Kcnk9KO</i> ^{mat} 5.307 ± 0.6183 5.963 ± 0.1874 6.738 ± 0.2760	DMSO VPA DZnep SAHA CI-994	7 3 3 3 3	one way ANOVA	Bonferroni's multiple comparisons test vs. DMSO ***P < 0.0001 F (4, 14) = 92.00 P < 0.0001 ***P < 0.0001 ***P < 0.0001 ***P < 0.0001 ***P < 0.0001
Cortical neurons CI-994	4d		1.000 ± 0.0656 2.586 ± 0.3351 <i>Kcnk9KO</i> ^{mat} 3.642 ± 0.2920 4.349 ± 0.1035 5.216 ± 0.2264 3.636 ± 0.2824	DMSO 4 µM 20 µM 40 µM 80 µM WT DMSO	9 2 4 4 4 5	one way ANOVA	F (5, 22) = 75.51 P < 0.0001 Bonferroni's multiple comparisons test <i>Kcnk9KO</i> ^{mat} vs. DMSO ***P < 0.0001 ***P < 0.0001 ***P < 0.0001 ***P < 0.0001 ***P < 0.0001 ***P < 0.0001
Duration of unsilencing in cortical neurons	4e		1,000 ± 0,104 2,738 ± 0,339 <i>Kcnk9KO</i> ^{mat} 1,000 ± 0,089 2,619 ± 0,265	day 1 DMSO day 1 CI-994 day 10 DMSO day 10 CI-994	2 samples 3 samples 6 samples 4 samples	Unpaired t-test (Two-tailed)	1 day P=0,0297 10 days P=0,0001
Cortical neurons drugs no effect	Suppl. 3a		1.000 ± 0.0417 <i>Kcnk9KO</i> ^{mat} 0.901 ± 0.013 0.548 ± 0.338	DMSO Zebularine C646	7 3 4	Mann-Whitney U (Two-tailed)	vs. DMSO P=0,0667 P = 0,4727
RT-qPCR analysis of cluster genes	Suppl. 3b	<i>Kcnk9KO</i> ^{mat} <i>Eif2c2</i> <i>Chrac1</i> <i>Peg13</i> <i>Trappc9</i> <i>Kcnk9</i> <i>Eif2c2</i> <i>Chrac1</i> <i>Peg13</i> <i>Trappc9</i> <i>Kcnk9</i>	1,050 ± 0,014 0,646 ± 0,014 0,442 ± 0,018 0,337 ± 0,678 6,448 ± 0,016 2,718 ± 0,024 1,084 ± 0,024 1,060 ± 0,024 0,965 ± 0,608 20,870 ± 0,042	Cultures CI-994 20 µM CI-994 20 µM CI-994 80 µM CI-994 80 µM	2 3 3 3 2 3 2 3 3 2	Mann-Whitney U	
Neuron density after CI-994 treatment	Suppl. 3d		41,000 ± 4,082 <i>Kcnk9KO</i> ^{mat} 34,580 ± 3,530 34,860 ± 4,035	DMSO CI-994 10 µM CI-994 20 µM	12 9 9	one way ANOVA	F (2, 27) = 0.8983 P = 0.4191
RT-qPCR <i>Kcnk9</i> expression in several brain regions	5b		2.89 ± 0,20 1,18 ± 0,21 2.65 ± 0,55 2,22 ± 0,55 2,77 ± 0,41 2,01 ± 1,07 0,96 ± 0,19 2,08 ± 0,28	Cerebellum Cortex Hippocampus Pons Hypothalamus Medulla Prefrontal cortex Olfactory bulb	DMSO: 12 CI-994: 13 DMSO: 6 CI-994: 9 DMSO: 12 CI-994: 14 	Mann-Whitney U (Two-tailed)	P < 0.0001 P= 0,3251 P= 0.0003 P= 0,0002 P= 0,0003 P= 0,3961 P= 0,7319 P= 0,0022

Convent. ChIP		0.006498	\pm	0.002042		DMSO: 4		
H3K27ac	Suppl. 7j	H3K27ac fold change enrichment (Normalized to veh) in hippocampus of WT	1,606 1,000 1,094 1	\pm	0,351 0,290 0,210 0,2851	<i>kcnk9</i> prom <i>kcnk9</i> intron <i>Ig3</i>	CI-994: 4 DMSO: 4 CI-994: 4 DMSO: 4 CI-994: 4 DMSO: 4	P =0,2312 P =0,7998 P = 0,7092
			1,331	\pm	0,325			
			1	\pm	0,3143			

Abbreviations: n, number of samples/mice; n.s., not significant

Supplementary Table 2: Primers used for PCR and pyrosequencing analyses

Primer			Sequence (5' – 3')
TASK3-P3	F	Genotyping	TGCGAGCTTCAGAGAGGATG
TASK3-P4	R	Genotyping	ATGCTCTAATCTCCAGTCTG
Kcnk9 Exon2	F	Genotyping	CACCAAGCCATGTACTTCTC
Kcnk9 Exon2	R	Genotyping	GGACCGGAAGTAGGTGTTCC
Kcnk9-SNP	F	Allele-specific RT-qPCR	CACAACTATCGGATATGGACATGC
Kcnk9-SNP	R	Allele-specific RT-qPCR	TGCCGCGGTGTTCGAT
Kcnk477	F	QUASEP	GCCTGTACCTCACCTAC
Kcnk477	R	QUASEP	CACAACTATCGGATATGGACATGC
Kcnk477_S	Seq	QUASEP	TGCCGCGGTGTTTC
kcnk9-283/284	F	RT-qPCR	ACTATCGGATATGGACATGCTGC
kcnk9-283/284	R	RT-qPCR	GCCCAGGCTCTGAAACATAA
Bdnf	F	RT-qPCR	ATCCACTGAGCAAAGCCGAA
Bdnf	R	RT-qPCR	CCTGGTGGAACATTGTTGGCT
Impa2	F	RT-qPCR	CGTGGGGACAAATCATCAG
Impa2	R	RT-qPCR	AAGGAAACCGCTTCGCAAC
Kcnk9 promoter	F	ChIP-qPCR	CGTGTGCGCTACATCTCTTA
Kcnk9 promoter	R	ChIP-qPCR	ATTGCCGGTCTCTTCTACT
Kcnk9 intron	F	ChIP-qPCR	AGGGCAGATGCTTAAGAGGA
Kcnk9 intron	R	ChIP-qPCR	CATCTGTTCTGTACCCCCATCC
mPeg13-CpG 1-9	F	Methylation analysis	TTGGATGAGTTATTATATAAGGTTAAAA
mPeg13-CpG 1-9	R	Methylation analysis	ACAACTACCTACATTCCAAATCT
mPeg13-CpG_1-9	Seq	Methylation analysis	AAATTAAATAAGATGGGTTAAT
mPeg13-CpG 17-22	F	Methylation analysis	AGATTGGAATGTAGGTAGTTGTGA
mPeg13-CpG 17-22	R	Methylation analysis	CCTCAATAAAACCATTCTAATCAACTAT
mPeg13-CpG 17-22	Seq	Methylation analysis	GGTAATTGTTAGGTGGAGATATA
Ago2_F	F	Cluster gene analysis	CGACACATCACCCATCCCA
Ago2_R	R	Cluster gene analysis	TTTGATTGTTCTCCGGTGGT
Chrac1_F	F	Cluster gene analysis	AAGAGCTCTCCGAGGTGTC
Chrac1-R	R	Cluster gene analysis	TACTGAACAAAGAGCTCCGTGGC
Peg13_F	F	Cluster gene analysis	AAGATCCGCGGCCTTACTC
Peg13_R	R	Cluster gene analysis	TTTGCCCATTCTCGGTCA
Trappc9_F	F	Cluster gene analysis	TGGGGCTGAAAAGACACTACAA
Trappc9_R	R	Cluster gene analysis	TGGTAGTGTACCAGGGCGT
Kcnk9-SNP_EP-C_F	F	AS-RT-qPCR	TGCCGCGGTGTTCGAC
Kcnk9-SNP_EP_R	R	AS-RT-qPCR	GCATGTCCATATCGATAGTTGTG
Kcnk9-SNP_EP-T_F	F	AS-RT-qPCR	TGCCGCGGTGTTCGAT
KCNK9-AS-ChIP-F	F	AS-CHIP	AAATTGCGCGGTCTCTTCTAC
KCNK9-AS-ChIP-R	R	AS-CHIP	gagatgtacgcacacgaagc
KCNK9-AS-ChIP-S	Seq	AS-CHIP	aaggaaatgggtgtgc

Abbreviations: F, forward primer; R, reverse primer; Seq, pyrosequencing primer

Supplementary References

1. Paxinos, G. & Franklin, K. B. J. *The Mouse Brain in Stereotaxic Coordinates* (Academic Press, 2008).